IMPLICIT AND EXPLICIT SENSITIVITIES FOR OPTIMIZATION OF COOLED TURBINE BLADES

Thomas J. Martin
Systems Engineer. Member AIAA
Turbine Discipline Engineering & Optimization Group
Pratt & Whitney Engine Company, 400 Main Street, MS 165-16, East Hartford, CT 06108
(860) 557-2585 (phone) (860) 557-2867 (FAX) martintj@pweh.com

George S. Dulikravich
Professor and Director. Associate Fellow AIAA.
Multidisciplinary Analysis, Inverse Design, and Optimization (MAIDO) Center
Department of Mechanical and Aerospace Engineering, UTA Box 19018
The University of Texas at Arlington, Arlington, Texas 76019
(817) 272-7376 (phone) (817) 272-5010 (FAX) dulikra@mae.uta.edu

ABSTRACT

The partial derivatives of field variables (temperatures, temperature gradients, thermal conductivity, heat sources. etc.) and boundary values (heat fluxes, heat transfer coefficients, heat radiation, etc.) with respect to the perturbations of the boundary conditions and geometry are very useful when performing a parametric study of a particular design. These partial derivatives are called design sensitivity coefficients. The implementation of gradient-based algorithms for inverse thermal shape design and numerical optimization require these partial derivatives as part of their operation. But the computer generation of these sensitivity coefficients can use up a great deal of computer resources and processing time. In order to make computer-automated optimization practicable in the design environment of the highly competitive turbomachinery industry, any reduction in resources, time and manpower should be attempted. Implicit differentiation of the aerodynamic, structural and thermal simulation codes can provide a significant reduction in the computer-processing time, resulting in faster turn-around times by the optimization team. It makes the use of optimization in the standard design practices of the company not only viable, but also it can reduce the design cycle time, achieve an optimal design, and make the company more competitive.

I. METHODS OF CALCULATING DESIGN SENSITIVITY COEFFICIENTS

In general, there are at least four methods that can be used to determine sensitivity coefficients: 1) analytical differentiation, 2) numerical differentiation by finite differencing, 3) direct implicit differentiation of the governing equations and 4) the adjoint operator method. The second method, finite differencing, is the simplest, most common and most expensive strategy of obtaining sensitivity coefficients. It requires, at a minimum, the brute force solution of the governing system(s) once for every design variable with first order forward or backward differencing formulas. This assumes that the original design, V_i, had already been evaluated. If second-order accuracy with central differencing is desired, the governing system must be evaluated twice per every design variable. The forward and central differencing formulas can be expressed as follows.

$$\left(\frac{\partial F}{\partial V_i}\right)_F = \frac{F(V_i + \Delta V_i) - F(V_i)}{\Delta V_i}$$

$$\left(\frac{\partial F}{\partial V_i}\right)_C = \frac{F\left(V_i + \Delta V_i\right) - F(V_i - \Delta V_i)}{\Delta V_i} \qquad (1)$$

The finite differencing method for sensitivity calculations can be prohibitively expensive, especially when the optimization concerns complex three-dimensional problems and finely discretized grids.

The third method involves the implicit differentiation of the equations at the system level. Considerable effort has been applied to these techniques and they have been used extensively for the efficient implementation of shape optimization of large-scale structures[1]. Implicit differentiation offers a practical design sensitivity calculation because the factorization of the big coefficient matrix needs to be performed only once and stored. In addition, implicit differentiation have been found to be more accurate than explicit finite differencing[2,3]. Kane and Saigal[4] obtained their sensitivity coefficients by differentiating the coefficient matrices formed by the boundary integral equations of two-dimensional sub-structural problems. This method has been extended to three-dimensional elasticity problems[5], and to thermo-elasticity[6]. This research effort utilizes an implicit design sensitivity formulation of the governing BEM heat conduction system that was based on the efforts of these researchers[7,8].

The fourth method has been referred to as the adjoint operator method[9,10] or the continuum approach. It uses variational concepts such as the material derivative[11]. By defining an adjoint problem, the sensitivity coefficients are found in terms of the primary and adjoint variables, thus requiring only the solution of one primary system and one adjoint system to obtain the gradient with respect to every design variable[12]. .

The adjoint operator method has several drawbacks. First, the adjoint variable method requires a very complicated formulation of the optimization problem that needs to be developed uniquely for each objective and constraint function. Thus, an entirely new system of partial differential equations must be developed for each function in terms of some non-physical adjoint variables and boundary conditions. Although it has been proven successful with finite elements, the BEM version of the adjoint variable method was found to be less satisfactory because the approximate adjoint tractions (or fluxes) could not be specified uniquely[11]. Due to these facts, as well as its lack of generality and overall decreased accuracy versus implicit differentiation, only finite differencing and implicit differentiation will be reported in this research.

II. IMPLICIT DIFFERENTIATION OF BEM HEAT CONDUCTION SYSTEM

The BEM is based upon the Green's function solution procedure. The boundary integral equation (BIE) for two- and three-dimensional heat conduction is well known[13].

$$c(x)T(x)+\int_{\Gamma} q^*(x,x)T(x)\,d\Gamma(x)=\int_{\Gamma} u^*(x,x)q(x)\,d\Gamma(x) \tag{2}$$

Since we are strictly solving a boundary value problem, the unknown temperature function $T(x)$ is only on the boundary Γ. The system of boundary integral equations for heat conduction (Equation 2) was differentiated with respect to the vector of optimization design variables, V_i.

$$\begin{aligned}
&\frac{\partial c(x)}{\partial V_i}T(x)+c(x)\frac{\partial T(x)}{\partial V_i}+\int_x \frac{\partial q^*(x,x)}{\partial V_i}T(x)\left|\bar{h}\right|dx\\
&+\int_x q^*(x,x)\frac{\partial T(x)}{\partial V_i}\left|\bar{h}\right|dx+\int_x q^*(x,x)T(x)\frac{\partial\left|\bar{h}\right|}{\partial V_i}dx\\
&=\int_x \frac{\partial u^*(x,x)}{\partial V_i}q(x)\left|\bar{h}\right|dx+\int_x u^*(x,x)\frac{\partial q(x)}{\partial V_i}\left|\bar{h}\right|dx\\
&+\int_x u^*(x,x)q(x)\frac{\partial\left|\bar{h}\right|}{\partial V_i}dx
\end{aligned} \tag{3}$$

Here, x is a localized contour or surface area coordinate and $\left|\bar{h}\right|$ is the Jacobian of the contour or surface integral. The chain rule was used on all quantities affected by the design variable, V_i. The derivatives of the three types of boundary conditions were found in the same way.

Dirichlet
$$\overline{\frac{\partial T}{\partial V_i}}=0 \tag{4}$$

Neumann
$$\overline{\frac{\partial q}{\partial V_i}}=0 \tag{5}$$

Robin

$$\begin{aligned}
&-k\frac{\partial q}{\partial V_i}-\frac{\partial k(T)}{\partial T}\frac{\partial T}{\partial V_i}q\\
&=\frac{\partial h}{\partial V_i}(T-T_{amb})+h\left(\frac{\partial T}{\partial V_i}-\frac{\partial T_{amb}}{\partial V_i}\right)
\end{aligned} \tag{6}$$

Here, h refers to the external or internal heat transfer coefficients and T_{amb} refers to the ambient temperature, which is either the turbine inlet total temperature, the external adiabatic wall temperature or the bulk total temperature of the coolant. After discretization of the BIEs, but before the application of boundary conditions, the linear algebraic system for heat conduction design sensitivity was expressed in the following matrix form

$$[d\mathbf{C}/d\mathbf{V}]\{\mathbf{T}\}+[\mathbf{C}]\{d\mathbf{T}/d\mathbf{V}\}+[d\mathbf{H}/d\mathbf{V}]\{\mathbf{T}\}$$

$$+[\mathbf{H}]\{d\mathbf{T}/d\mathbf{V}\} = [d\mathbf{G}/d\mathbf{V}]\{\mathbf{Q}\}+[\mathbf{G}]\{d\mathbf{Q}/d\mathbf{V}\} \qquad (7)$$

This equation is valid for both two- and three-dimensional domains. The vectors of nodal temperatures, **{T}**, and heat fluxes, **{Q}**, are already known from the previous analysis of the temperature field at the current design point. The coefficient matrices **[C]**, **[G]**, and **[H]** are also known if they were stored into computer memory.

There are two possible ways of determining the differentiated coefficient matrices, [d**C**/d**V**], [d**G**/d**V**], and [d**H**/d**V**]. In most implicit differentiation methodologies using the BEM, the derivatives of the fundamental solution that appear in the preceding equation are calculated implicitly from the spatial derivative in the $\vec{x}$ and $\vec{x}$ coordinate systems [5], where $r = \left|\vec{x} - \vec{x}\right|$.

$$\frac{\partial u^*}{\partial V_i} = \frac{\partial u^*}{\partial x_m}\left(\frac{\partial x_m}{\partial V_i} - \frac{\partial x_m}{\partial V_i}\right) \qquad (8)$$

Unfortunately, these integrands result in hyper-singular fundamental solutions of the order *1/r* and $1/r^2$ in two-dimensional problems, and $1/r^2$ and $1/r^3$ and in three-dimensional problems, resulting in the need for very special integration methods. The rigid body assumption can be used to compute some weakly singular integrals that occur when the source and field points coincide but, in general, special methods are needed. Hyper-singular integration techniques are complex, requiring Laurent series expansions of the hyper-singular integrand about the singular point and a transformation to a local polar coordinate system in three-dimensional problems [14,15].

Although hyper-singular integration is difficult to program and time-consuming, significant computational savings can be realized because the numerical integration of the differentiated fundamental solutions needs to be performed only twice for two-dimensional problems and three times for three-dimensional problems. Finite differencing of the boundary contours or surfaces, $\partial x_m / \partial V_i$, would still be necessary if the design variables could not be expressed as closed form functions of the boundary contour or surface parameters.

In this research, hyper-singular integration has been avoided for a slightly more expensive method of finite differencing the coefficient matrices [d**H**/d**V**] and [d**G**/d**V**].

$$\left[\frac{\partial \mathbf{H}}{\partial V_i}\right] = \frac{[\mathbf{H}(V_i + \Delta V_i)] - [\mathbf{H}(V_i)]}{\Delta V_i} \qquad (9)$$

The boundary needs to be integrated for the initial geometry and stored, and then it needs to be integrated once for every design variable perturbation. The finite differencing formula (9) can then be applied. Its only advantage over hyper-singular integration is that it is very easy to program. Since most computing time is involved in the factorization of the coefficient matrix [**A**], rather than during the integration over the boundary, this method still provided a substantial reduction in computing time at the expense of the memory required to store two sets of BEM coefficient matrices. When the memory requirements are very large, these coefficient matrices could not be stored into random access memory. Instead, they were written and read from the workstation's hard drive.

Ultimately, the linear system of equations were solved for the unknown derivatives of temperature and heat flux $\partial T/\partial V_i$ and $\partial q/\partial V_i$. These unknowns were cast into the vector **{dX/dV}** and solved for by multiplying the previously factored BEM matrix, $[\mathbf{A}]^{-1}$. It should be pointed out that the inversion of the coefficient matrix, [**A**], does not change from the heat conduction analysis of the original design.

$$[\mathbf{A}]^{-1}\left\{\frac{\partial \mathbf{X}}{\partial V_i}\right\} = -[\mathbf{H}']\{\mathbf{T}\} + [\mathbf{G}']\{\mathbf{Q}\} + \left\{\frac{\partial \mathbf{F}}{\partial V_i}\right\} \qquad (10)$$

III. GRADIENTS OF THE OBJECTIVE FUNCTIONS

The gradients of each thermal objective function were computed given the thermal sensitivity coefficients, $\partial T/\partial V_i$ and $\partial q/\partial V_i$. These quantities were then used in the differentiated objective functions where they were applicable.

Analytic Gradients of the Specific Thrust and Turbine Efficiency

The ideal cycle analysis for a turbojet engine yields the following closed form expression for the specific thrust at cruise[16].

$$F(\vec{V}) = \frac{T}{\dot{m} a_\infty} = \sqrt{\frac{q_\infty}{q_\infty - 1}\left(\frac{q_t}{q_\infty t_c} - 1\right)(t_c - 1) + \frac{q_t}{q_\infty t_c} - 1} \qquad (11)$$

where $\dot{m}$ is the mass flow rate of the primary engine airflow.

$$q_\infty = \left(1 + \frac{g_\infty - 1}{2} M_\infty^{\,2}\right) \qquad q_t = \frac{T_{t,inlet}}{T_\infty} \tag{12}$$

In these equations, M_∞ is the flight Mach number, T_∞ is the static temperature of the ambient air at cruise altitude, t_c is the stagnation temperature ratio of the compressor and g is the ratio of specific heats, which is assumed to be constant in this expression. During numerical optimization of the ideal specific thrust of a turbojet, the implicitly-differentiated gradient of Equation 11 is only sensitive to the turbine inlet total temperature, $T_{t,inlet}$. This gradient is unaffected by the internal cooling scheme and, as such, it is independent of the heat conduction in the turbine blades.

$$\frac{\partial F(\vec{V})}{\partial T_{t,inlet}} = \frac{M_\infty \left[\left(\frac{q_\infty}{q_\infty - 1}\right)\frac{(t_c - 1)}{q_\infty t_c T_\infty} + \frac{1}{q_\infty t_c T_\infty}\right]}{2\sqrt{\left(\frac{q_\infty}{q_\infty - 1}\right)\left(\frac{q_t}{q_\infty t_c} - 1\right)(t_c - 1) + \frac{q_t}{q_\infty t_c}}} \tag{13}$$

In a real turbojet engine without internal cooling (see Equation 11), the specific thrust was also sensitive to the adiabatic turbine efficiency[16], h_t. The analytic differentiation of Equation 11 required knowledge of the sensitivity of the turbine efficiency, but h_t is a function of the aerodynamics, not the heat conduction. It was too difficult to implicitly differentiate the CFD program[17] (RVQ3DN) for the sensitivity coefficients of an aerodynamic turbine efficiency optimization. Therefore, finite differencing formulas were used to calculate $\partial h_t / \partial T_{t,inlet}$. Equation 11 was analytically differentiated with respect to the turbine inlet total temperature and a closed form expression similar to Equation 14 was employed. This equation was independent of both the heat conduction and the internal coolant pressure losses and heat-up.

$$\frac{\partial F(\vec{V})}{\partial T_{t,inlet}} = \frac{\sqrt{1 - \frac{1}{q_\infty p_t^{\,(g-1)/g}\left[1 + h_c(t_c - 1)\right]\left[1 - \frac{q_\infty(t_c - 1)}{h_t q_t}\right]}}}{2T_\infty\sqrt{q_\infty - 1}\sqrt{q_t - q_\infty(t_c - 1)}} - \\ - \sqrt{\frac{q_t - q_\infty(t_c - 1)}{q_\infty - 1}} \times$$

$$\frac{q_\infty p_t^{\,(g-1)/g}\left[1 + h_c(t_c - 1)\right] q_\infty(t_c - 1)\left\{\frac{1}{h_t q_t^{\,2} T_\infty} + \frac{\partial h_t / \partial T_{t,inlet}}{h_t^{\,2} q_t}\right\}}{\left\{q_\infty p_t^{\,(g-1)/g}\left[1 + h_c(t_c - 1)\right]\left[1 - \frac{q_\infty(t_c - 1)}{h_t q_t}\right]\right\}^{3/2}} \\ \overline{2\sqrt{q_\infty p_t^{\,(g-1)/g}\left[1 + h_c(t_c - 1)\right]\left[1 - \frac{q_\infty(t_c - 1)}{h_t q_t}\right] - 1}} \tag{14}$$

Cooled Turbine Efficiency. It is defined as the ratio of the actual turbine work per unit of total air flow (primary, plus cooling) divided by the ideal work that would be achieved by expanding that total airflow through the actual pressure ratio. The ratio of the cooling airflow to total airflow is given[16] by $f_c = \dot{m}_c / \dot{m}$. Hence, the cooled turbine efficiency is

$$h_{tt} = \frac{(1 - f_c)(T_{t,inlet} - T_{t,exit}) + f_c(T_{t,c} - T_{t,exit})}{\left[(1 - f_c)T_{t,inlet} + f_c T_{t,c}\right]\left[1 - \left(p_{t,exit}/p_{t,inlet}\right)^{(g-1)/g}\right]} \tag{15}$$

Here, $T_{t,c}$ is the inlet total temperature of the cooling air. Given a coolant flow to hot gas flow ratio, f_c, and total temperature ratio across the turbine, the cooled turbine efficiency can be used to calculate the total pressure ratio ($p_{t,exit}/p_{t,inlet}$). The cooled turbine efficiency, h_{tt}, is sensitive to most, if not all, of the design variables.

$$\frac{\partial h_{tt}}{\partial V_i} = \frac{\frac{\partial f_c}{\partial V_i}(T_{t,c} - T_{t,inlet}) + f_c\left(\frac{\partial T_{t,c}}{\partial V_i} - \frac{\partial T_{t,exit}}{\partial V_i}\right) + B}{\left[(1 - f_c)T_{t,inlet} + f_c T_{t,c}\right]\left[1 - \left(p_{t,exit}/p_{t,inlet}\right)^{(g-1)/g}\right]} \\ - \frac{A\left[(1 - f_c)(T_{t,inlet} - T_{t,exit}) + f_c(T_{t,c} - T_{t,exit})\right]}{\left[(1 - f_c)T_{t,inlet} + f_c T_{t,c}\right]^2\left[1 - \left(p_{t,exit}/p_{t,inlet}\right)^{(g-1)/g}\right]}$$

$$A = (1 - f_c)\frac{\partial T_{t,inlet}}{\partial V_i} + \frac{\partial f_c}{\partial V_i}(T_{t,c} - T_{t,inlet}) + f_c\frac{\partial T_{t,c}}{\partial V_i}$$

$$B = (1 - f_c)\left(\frac{\partial T_{t,inlet}}{\partial V_i} - \frac{\partial T_{t,exit}}{\partial V_i}\right) \tag{16}$$

$T_{t,inlet}$ is only sensitive to itself, and thus is equal to 1.0 when $V_i = T_{t,inlet}$, and it is zero for all other design variables. $T_{t,c}$ is the inlet stagnation temperature of

the coolant air, which is either a design variable, or it is related only to the inlet stagnation pressure of the coolant air, $P_{t,c}$, which itself is a design variable.

The adiabatic compression equation was used for the relationship between inlet coolant static temperature, $T_{t,c}$, and the static pressure, $P_{t,c}$, for an ideal compressor.

$$\frac{p}{r^{g}} = p^{1-g} R^{g} T^{g} = constant \tag{17}$$

The inlet coolant conditions are related to the compressor bleed total pressure, $P_{t,3}$, and total temperature, $T_{t,3}$, by this equation. In the former case, it is differentiated in the same way as $T_{t,inlet}$. In the latter case, Equation 17 was analytically differentiated with respect to $P_{t,c}$.

$$\frac{\partial T_{t,c}}{\partial P_{t,c}} = p_{\infty}^{1-g} T_{\infty}^{g} (g-1) P_{t,c}^{g-2} \tag{18}$$

Again, $p_{t,exit}$ and $T_{t,exit}$ are the spanwise and circumferentially averaged total pressure and temperature at the exit plane of the turbine. The turbine exit total pressure was a function of the aerodynamics so its sensitivity was calculated by finite differencing the CFD solutions. For a fixed external blade shape, it was assumed that exit total pressure, $p_{t,exit}$, was fixed with respect to the cooling scheme design variables, so its sensitivity was ignored.

For a closed-loop internal cooling system and a given temperature drop in the turbine, the loss of heat to the coolant air, Q_c, reduces the amount of work that can be extracted by the turbine, and this directly reduces the available shaft power, P_S.

$$\begin{aligned} &(\dot{m} - \dot{m}_c + \dot{m}_f) c_{pt} T_{t,inlet} \\ &= (\dot{m} - \dot{m}_c + \dot{m}_f) c_{pt} T_{t,exit} + P_S + Q_c \end{aligned} \tag{19}$$

In closed loop cooling systems, the heat transfer to the coolant reduces the turbine efficiency. Therefore, the sensitivity of the exit total temperature, $\partial T_{t,exit} / \partial V_i$ is a function of the heat flux sensitivity, $\partial Q_c / \partial V_i$ that is calculated by the implicit BEM.

$$\frac{\partial T_{t,exit}}{\partial V_i} = \frac{(\dot{m} - \dot{m}_c) c_{pt} \dfrac{\partial T_{t,inlet}}{\partial V_i}}{(\dot{m} - \dot{m}_c) c_{pt}} - \frac{\dfrac{\partial \dot{m}_c}{\partial V_i} c_{pt} (T_{t,inlet} - T_{t,inlet}) - \dfrac{\partial Q_c}{\partial V_i}}{(\dot{m} - \dot{m}_c) c_{pt}} \tag{20}$$

But, when the heated coolant air is ejected and mixed with the hot combustion product gases and expanded to the turbine exit stagnation temperature, $T_{t,exit}$, the heat flux absorbed by the turbine blades is transferred to the working fluid. Then, the shaft power is the same as that used for the actual work in the cooled turbine efficiency equation.

$$\begin{aligned} &(\dot{m} - \dot{m}_c + \dot{m}_f) c_{pt} T_{t,inlet} + \dot{m}_c c_{pc} T_{t,c} \\ &= (\dot{m} + \dot{m}_f) c_{pt} T_{t,exit} + P_S \end{aligned} \tag{21}$$

Here, the addition of the heated cooling air to the hot gas flow increases the shaft power. Since this paper deals with cooled aircraft turbines where the work extracted by the turbine was fixed during the internal cooling passage optimization, there was no sensitivity of $T_{t,exit}$ to the design variables.

The coolant airflow ratio, f_c, is directly proportional to the pressure losses in the coolant flow passages. Thus, it is sensitive to the total pressure of the coolant, $P_{t,c}$, the heat transfer enhancement parameters (i.e. trip strip height and spacing, tube bank diameter, etc.) and the static pressures where the coolant air dumps to the hot gas flow. Therefore, $\partial f_c / \partial V_i$ was determined using finite differencing. Since the internal coolant flow solver runs very quickly, this is not a serious flaw.

Thus, Equations 14, 16 and 18 can be used to provide mixed analytical/finite differenced design sensitivities of the internal turbine blade cooling objective functions. Note that the specific thrust, as specified in equation 11, is insensitive to the internal turbine blade cooling design variables.

Implicit Differentiation of the Cooling Effectiveness For internal convective cooling schemes, an optimization objective can be mathematically formulated as the maximization of the cooling effectiveness or convective efficiency.

$$F(\vec{V}) = f = \int_{\Gamma_E} \frac{T_G - T}{T_G - T_{t,c}} d\Gamma \tag{22}$$

In this equation, T_G is the external hot gas or adiabatic wall temperature, $T_{t,c}$ is the total temperature of the coolant at the inlet to the coolant passages, T is the metal temperature, and Γ_E indicates integration over the external surface of the turbine

blade. Maximization of this objective function drives the temperature of the turbine blade or vane towards the coolant temperature, thus improving its durability. The sensitivity of the cooling effectiveness was determined by implicit differentiation of Equation 22.

$$\frac{\partial F}{\partial V_i} = \frac{\partial f}{\partial V_i} = \int_x \left\{ \frac{(T_G - T)}{(T_G - T_{t,c})} \frac{\partial |\vec{h}|}{\partial V_i} \right\} dx + \int_x \left[\frac{\left(\frac{\partial T_G}{\partial V_i} - \frac{\partial T}{\partial V_i} \right)}{T_G - T_{t,c}} - \frac{(T_G - T)\left(\frac{\partial T_G}{\partial V_i} - \frac{\partial T_{t,c}}{\partial V_i} \right)}{(T_G - T_{t,c})^2} \right] |\vec{h}| dx \quad (23)$$

In the cooling effectiveness equation, T_G is the external gas temperature, which is either the turbine inlet total temperature or the adiabatic wall temperature. The sensitivity of $T_{t,c}$ was calculated by Equation 18 and $\partial T / \partial V_i$ was calculated by the implicit BEM system (Equation 7).

Implicit Differentiation of the Corrosion Objective The corrosion effect may be represented by a constraint function in order to make sure that extreme metal temperatures do not exist in the metal. Equation 24 represents an equality constraint function that can maintain blade life limited by oxidation and sulfidation.

$$F(\vec{V}) = \int_{\Omega_M} (T - T_{SuOx})^2 d\Omega \qquad H(\vec{V}) = |T - T_{SuOx}|_{max} \le d_T \quad (24)$$

Here, T_{SuOx} is the target temperature that corresponds to a local maximum of the blade alloy life with respect to oxidation and corrosion. Equation 24 was differentiated with respect to the design variable vector, V_i, in order to obtain the gradient of the oxidation/sulfidation function.

$$\frac{\partial F}{\partial V_i} = \int_{\Omega} 2(T - T_{SuOx}) \frac{\partial T}{\partial V_i} d\Omega \quad (25)$$

Gradients of the Thermal Constraint Functions Potentially greater savings of computational resources can be achieved with the use of implicit differentiation for the computation of gradients of the constraint functions. Implicit differentiation of the constraint function yields substantial savings because of the ability to re-use the previous inversion of the BEM coefficient matrix, $[A]^{-1}$. A BEM solution of the non-linear heat conduction equation is required for every constraint function analysis just as for the thermal objective function analysis. When the constraints are active or violated, the gradient of the constraint functions with respect to the design variables are needed in order to project the searching directions. Therefore, these gradient calculations are needed more often for the gradient-based constraint restoration procedures that restore infeasible designs back to feasibility[18]. Two constraint functions were employed within our turbine blade cooling optimization system, corrosion (see Equation 24) and thermal integrity.

Implicit Differentiation for Thermal Integrity For thermally-constrained shape optimization problems, the temperature field needs to be computed in order to determine the maximum temperature. The implicitly differentiated inequality and equality constraint function has the following form.

$$\frac{\partial G}{\partial V_i} = \frac{1}{T_{max}} \frac{\partial T}{\partial V_i} \Bigg\}_{@T_{max}} \quad (26)$$

THERMAL OPTIMIZATION OF AN INTERNALLY COOLED STRUT AIRFOIL

The potential practical benefits of using implicit differentiation for design sensitivity analysis has been demonstrated on a two-dimensional thermal optimization problem of a symmetric internally cooled configuration. A Rankine oval shape (Figure 1) that had an axial chord of 2.0 m and a thickness of 0.2 m was chosen to simulate a support strut airfoil while its symmetry throughout the geometric shape optimization procedure would demonstrate the accuracy of the method. The internally cooled strut airfoil was modeled as being made of stainless steel with thermal conductivity k = 30.0 $Wm^{-1}K^{-1}$ and having a 150 microns thick thermal barrier coating with thermal conductivity k = 1.0 Wm^{-1} K^{-1}. Twenty geometric design variables and six boundary condition design variables were used to develop the internally cooled strut airfoil design. These are listed and described again for clarity in Table 1.

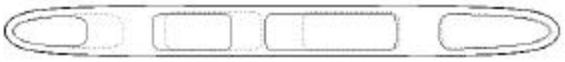

Figure 1. Rankine oval shape for the symmetric example of a strut airfoil, with optimization starting point (dotted lines) and final optimized (solid lines) shapes of the coolant passages.

The four coolant flow passages were initially symmetrically sized and located. Coolant heat transfer coefficients, h_c, and bulk temperatures, $T_{t,c}$, were applied as boundary conditions to the internal walls of the four coolant passages. The objective of this example problem was the uniform target temperature function represented by the oxidation/sulfidation minimization objective in Equation 24. The desired target temperature in the strut airfoil was specified to be $T_{SuOx}=1300\ K$. This optimization problem was constrained by the maximum temperature constraint (equation 24) where $\overline{T_{max}}=1375\ K$ The conjugate aero-thermo-fluid analysis started with constant temperature on the external wall of the strut airfoil.

Table 1. Numbers and descriptions of design variables used in thermal optimization problem of an internally cooled strut airfoil.

Number	*Total*	*Description*	*Symbol*
8	8	β-spline vertices for the coolant wall thickness function	*W(V(s))*
2 per strut	6	x-locations for each strut	x_{SP},x_{SS}
1 per strut	3	thickness for each strut	t_S
1 per strut	3	super-elliptic exponent for strut filleting	e_S
1	1	coolant mass flow rate	G
1	1	hot gas turbine inlet temperature	T_{inlet}
1 per hole	4	coolant wall roughnesses (trip strip height)	e

Table 2. CFD boundary conditions applied to the rotor viscous quasi-three-dimensional flow solver for the subsonic flow over a Rankine oval strut airfoil.

Property	*Value & Units*
$P_{t,inlet}$	225,000.0 N/m^2
$T_{t,inlet}$	1500.0 K
	200,000.0 N/m^2
T_{wall}	1200.0 K
V_{inlet}	150 m/s
a_{le}	0.0^o

A structured viscous quasi-three-dimensional CFD code[17] for turbine rotor blades was used to predict the corresponding temperature derivatives normal to the surface. This code used the Baldwin-Lomax turbulence model with a turbulent Prandtl number of *0.9*. A list of the boundary conditions applied to this CFD run is given in Table 2.

The hot gas computational region was represented by a G-grid having *140 x 30* grid cells clustered towards the airfoil with a grid cell layer adjacent to the wall having a turbulent $y^+=5.0$. Sutherland's formula was used for the fluid viscosity and the hot gas was assumed to be air.

Using the flexible geometry treatment of the interior of the airfoil, and using a conjugate heat transfer analysis between the external hot gas flow and the heat conduction in the airfoil, the objective function was developed and the four coolant flow passages were modified and converged to their new shapes and locations (Figure 1). Given the hot gas ambient temperature, $T_{t,inlet}$, a heat convection coefficient distribution was obtained from the heat fluxes into the solid strut. The temperature distribution on the outer airfoil surface was more uniform than the initial surface temperature distribution and the stagnation point temperature was decreased slightly (Figure 2). At the same time, the optimized coolant passages allowed for a significantly higher inlet hot gas temperature (Figure 3) and a lower coolant mass flow rate (Figure 4). The coolant pressure loss (Figure 5) in the coolant channels increased because of the need for the increased relative surface roughness (Figure 6) for increased heat transfer coefficients (Figure 7) on the walls of the coolant passages.

The internal cooling optimization was performed using our hybrid constrained optimization algorithm[18] and was executed with and without implicit thermal design sensitivity. In the latter case, forward finite differencing was used for the objective function gradient. Both runs produced similar results, but the run using the implicit differentiation converged faster and to a lower minimum than did the explicit finite differencing run. This is demonstrated by the convergence history of the objective function in Figure 8. A comparison between the computing times on a single processor Cray C-90 from the explicit finite differenced and implicit differentiated design sensitivities for the entire optimization run is shown in Figure 9. This figure shows that there is a substantial reduction in the amount of computing time required, especially if one extrapolates the finite differencing result. Note that this dramatic improvement is the result of a two-dimensional example. Since the coefficient matrices of three-dimensional geometries are larger than two-dimensional matrices, the savings of computational resources are expected to be substantially greater for three-dimensional problems.

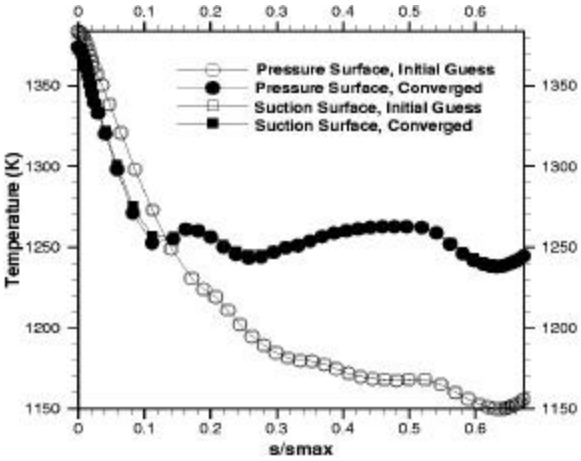

Figure 2. Temperatures computed by BEM on the outer airfoil surface of the strut airfoil.

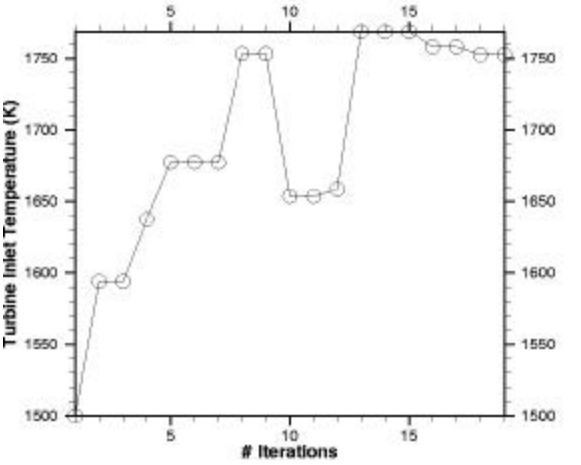

Figure 3. History of hot gas temperature during optimization of internal passages inside strut airfoil.

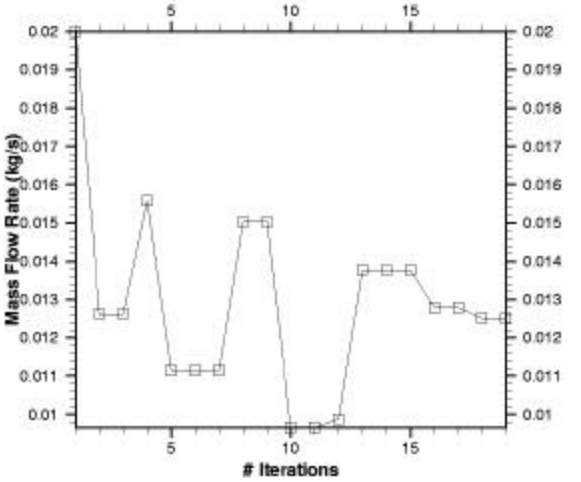

Figure 4. History of coolant mass flow rate design variable during optimization of an internally cooled strut airfoil.

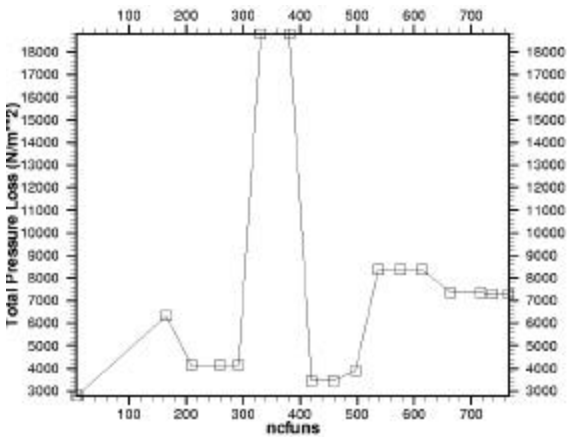

Figure 5. History of pressure loss in coolant channels during optimization of an internally cooled strut airfoil.

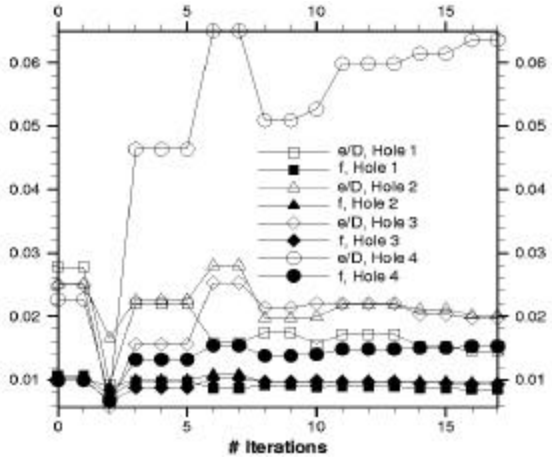

Figure 6. History of relative surface roughness during optimization of internal passages inside strut airfoil.

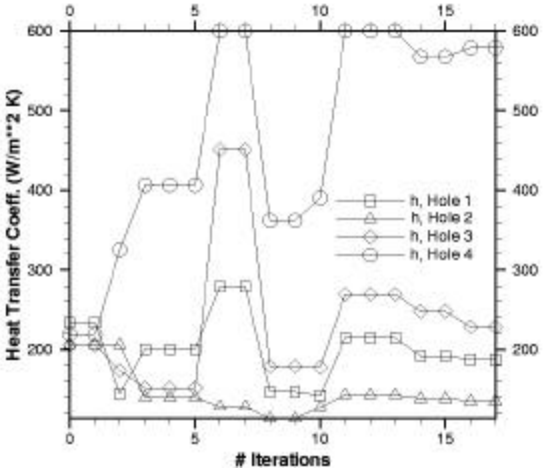

Figure 7. History of coolant heat transfer coefficients during optimization of an internally cooled strut airfoil.

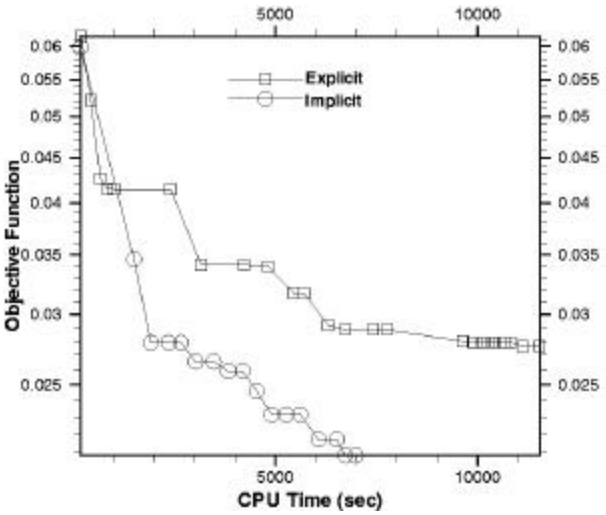

Figure 8. Convergence rates for explicit finite differencing and implicit differentiation. Each circle or square depicts one unconstrained optimization cycle.

FINITE DIFFERENCING VERSUS IMPLICIT DIFFERENTIATION

The accuracy of the implicit design sensitivity with the BEM was studied with respect to forward and central finite differences over a range of differencing step sizes. Gradients of the target temperature objective function (Equation 24) and maximum temperature constraint function (Equation 26) were determined at the optimization starting point of the Rankine oval constrained conjugate optimization problem. The perturbation step sizes, δ, for the implicit differentiation of the BEM coefficient matrices were the same as those for the finite differencing, and the magnitudes of the derivatives were compared over a range of δ ranging from 10^{-7} to 10^{-1}.

Understandably, central differencing was found to be far more accurate than forward differencing, and over a wider range of perturbation step sizes. Implicit differentiation of the BEM system was found to be just as accurate as central finite differencing, although over not as wide a range. The implicit gradients of the objective and constraint functions with respect to the geometric variables (beta spline vertex wall thickness, strut position, and strut thickness) were more accurate when there was a direct relationship between the change in the geometry and the objective function (e.g. wall thickness). The implicit differentiation method was also as accurate as the central differencing methods when the functions were differentiated with respect to the boundary condition design variables (wall roughness, boundary layer turbulator rib height, and internal coolant pressure loss). The boundary condition sensitivities were more accurate than the geometric sensitivities because truncation errors in the geometric definition were magnified more than the build up of round-off errors in the heat conduction solution. Naturally, truncation errors were larger with bigger differencing δ's, and round-off errors were larger with smaller δs. Unfortunately, the implicit derivatives tended to have a slight bias caused by the non-linearity of the boundary condition.

CONCLUSIONS

The multi-disciplinary (aerodynamically and thermally conjugate) optimization methodology that was presented here combined parametric geometry generation, computational aerodynamics, heat conduction and internal cooling fluid element software into a fully computer-automated design tool for the optimization of internally cooled turbine blades with thermal barrier coatings. The design process was controlled with a hybrid optimization algorithm in order to minimize a thermal optimization objective function subject to blade durability constraints. The minimization of the optimization objective function reflected an increase in turbine airfoil cooling effectiveness and/or durability while the turbine cooling scheme did not allow the maximum temperature to exceed the temperature limitations of the metal blade.

Implicit differentiation of the governing heat conduction system was programmed into the internally cooled turbine airfoil design and optimization system. Information from previous heat conduction calculations using the BEM (coefficient matrices and matrix factorizations) was saved into random access memory (RAM) and used for quick design sensitivity calculations. This provided substantial savings in computing time at the expense of increased computer memory requirements. Storing of the BEM coefficient matrices, matrix factorizations, and decompositions essentially doubled the required running memory.

Implicit differentiation was found to be more accurate than forward differencing, and just as accurate as central finite differencing, but truncation errors were larger with bigger differencing step sizes, and round-off errors were larger with smaller stepsizes. The boundary condition design variables were less sensitive to round-off errors than the geometry parameters, but the implicit derivatives tended to have a slight bias caused by the non-linearity of the boundary condition. With implicit differentiation, the computing time was reduced by a third for two-dimensional thermal optimizations and by at least a factor of twenty for three-dimensional thermal optimizations. This was because the matrix

factorization (or decomposition) was the most expensive process required of a BEM analysis.

The savings in computing time for three-dimensional thermo-elasticity optimizations is expected to be an order of magnitude larger, principally because the thermo-elastic BEM matrices are three times larger in dimension than the thermal matrices. Without implicit differentiation of the thermo-elastic system, realistic, three-dimensional aero-thermo-elastic optimization with the BEM would be prohibitively expensive at the present time.

REFERENCES

[1]Hafka, R. T. and Malkus, D. S., "Calculation of Sensitivity Derivatives in Thermal Problems by Finite Differences", *Int. Journal Numerical Methods in Engineering*., Vol. 17, 1981, pp. 1811-21.

[2]Aliabadi, M. H. and Mellings, S. C., "Boundary Element Formulations for Sensitivity Analysis and Crack Identification", *Boundary Integral Formulations for Inverse Analysis*, (ed. D. B. Ingham and L. C. Wrobel), Computational Mechanics Publications, 1997.

[3]Kane, J. H., Zhao, G., Wang, H., and Guru Prasad, K., "Boundary Formulations for Three-Dimensional Continuum Structural Shape Sensitivity Analysis", *Journal of Applied Mechanics*, Vol. 59, Dec. 1992, pp. 827-834.

[4]Kane, J. H. and Saigal, S., "Design Sensitivity Analysis of Solids Using BEM", *Journal of Engineering Mechanics*, ASCE, Vol. 114, No. 10, 1988, pp. 1703-1722.

[5]Yamazaki, K., Sakamoto, J., and Kitano, M., 'Three-Dimensional Shape Optimization Using the Boundary Element Method", *AIAA Journal*, Vol.32, No. 6, June 1994.

[6]Kane, J. H, Keshava-Kumar, B. L., and Stabinsky, M., "Transient Thermo-Elasticity and Other Body Force Effects in Boundary Element Shape Sensitivity Analysis", *Int. J. Numer. Methods Engr.*, Vol. 31, 1991, pp. 1203-1230.

[7]Martin, T. J., "Computer-Automated Multi-Disciplinary Analysis and Design Optimization of Internally Cooled Turbine Blades," Ph.D. dissertation, Aerospace Eng. Dept., Pennsylvania State University, University Park, PA, May 2001.

[8]Martin, T. J. and Dulikravich, G. S., "Aero-Thermo-Elastic Concurrent Design Optimization of Internally Cooled Turbine Blades", Chapter 5 in *Coupled Field Problems, Series on Advances in Boundary Elements* (eds: Kassab, A. J. and Aliabadi, M. H.), WIT Press, Boston, MA, 2001, pp. 137-184.

[9]Cabuk, H., Sung, C.-H. and Modi, V., "Adjoint Operator Approach to Shape Design for Internal Incompressible Flows", *Proc. of 3rd Intl. Conf. On Inverse Design Concepts and Optimization in Engr. Sci. (ICIDES-III)*, (ed. G. S. Dulikravich), Washington, D.C., Oct. 23-25, 1991, pp. 391-404.

[10]Reuther, J. and Jameson, A., "Control Based Airfoil Design Using the Euler Equations", *AIAA paper 94-4272-CP*, 1994.

[11]Meric, R. A., "Differential and Integral Sensitivity Formulations and Shape Optimization by BEM", *Engineering Analysis with Boundary Elements*, Vol. 15, 1995, pp. 181-188.

[12]Dulikravich, G. S., "Shape Inverse Design and Optimization for Three-Dimensional Aerodynamics", *AIAA Invited Paper 95-0695*, AIAA Aerospace Sciences Meeting, Reno, NV, Jan. 1995.

[13]Brebbia, C. A., *The Boundary Element Method for Engineers*, John Wiley & Sons, New York, 1978.

[14]Mikhilin, S. C., *Multidimensional Singular Integral Equations*, Pergamon Press, London 1965.

[15]Guiggiani, M., Krishnasamy, G., Rudolphi, T. J., and Rizzo, F. J., "A General Algorithm for the Numerical Solution of Hyper-Singular Boundary Element Integral Equations", *ASME Journal of Applied Mechanics*, Vol. 59, 1992, pp. 604-614.

[16]Kerrebrock, J. L., *Aircraft Engines and Gas Turbines*, MIT Press, Cambridge, MA, 1977.

[17]Chima, R. V., "Explicit Multigrid Algorithm for Quasi-Three-Dimensional Viscous Flows in Turbomachinery, *Journal of Propulsion and Power*, Vol. 3, No. 5, Sep.-Oct. 1987, pp. 397-405.

[18]Dulikravich, G. S., Martin, T. J., Dennis, B. H. and Foster, N. F.: "Multidisciplinary Hybrid Constrained GA Optimization", Chapter 12 in *EUROGEN'99 - Evolutionary Algorithms in Engineering and Computer Science: Recent Advances and Industrial Applications*, (eds: K. Miettinen, M. M. Makela, P. Neittaanmaki and J. Periaux), John Wiley & Sons, 1999, pp. 231-260.